# CHAPTER-II

# CHAPTER – II

# PREPARATION AND CHARACTERIZATION OF PYROCHLORES

## 2.1 INTRODUCTION: -

Most of the properties like Electrical, Thermal, optical and magnetic of pyrochlores depend on their porosity, microstructure and density. The porosity, microstructure and density of final product depend on the method of preparation. The properties of final product depends on purity of starting materials, mixing, sintering temperature and time, rate of cooling, part of pressure of oxygen inside the furnace. Also microstructure of factors such as defect concentration, inclusion of pores, grain size, grain shape and its orientation, considerably affects the properties of ceramic products. Hence to prepare best quality ceramic materials, standard method should be followed.

This chapter covers x-ray diffraction study under taken to confirm the formation of pyrochlores and method of preparation.

## 2.2 STANDARD CERAMIC METHOD OF PREPARATION: -

In the ceramic method very pure constituents in oxide form are taken in finely divided state. Then the constituents are thoroughly mixed uniformly using agate mortar or ball milling machine. The mixture is then presintered for 18–24 hrs. At temperature 700 – 900 °C (generally, presintering is carried out at temperature 50% of the M.P.), so as to facilitate solid state chemical reaction among the oxides and the formation of chemical compound. The presintered mixture is once again mixed uniformly using agate mortar or ball milling machine. Finally the mixture is sintered for 24 hours at temperature 1000 °c-1300 °C. (generally sintering temperature is 2/3 of the M.P.), so as to complete

the solid state chemical reaction among the oxides and the formation of chemical compound.

The ceramic method consists of following stages.

1 Thorough mixing of starting oxides taken in weighed amounts in stiochiometric proportion.

2 Presintering at the temperature slightly less than the solid state chemical reaction temperature.

3 Powdering and pressing to desire shape and

4 Final sintering and slow cooling up to room temperature.

All the details of the every stages involved are described in following sections. Fig. 2.1 shows flow chart of standard ceramic method.

**2.3 MIXING OF STARTING MATERIALS: -**

In order to get the best final product, the mixing of starting materials must be upto molecular scale. In order to achieve this, there are two methods, namely dry method and wet method.

**2.3.1 DRY METHOD: -**

Highly pure A.R. grade oxide materials are taken in required stiochiometric proportion and just blended physically. Then this mixture introduced into ball milling machine or agate mortar for several hours, with or without acetone as mixing medium. Continuous, random, vigorous and fast movement of balls in ball milling machine (or rotor in agate mortar) subjects the mixture to rapid attrition and mixes it homogeneously.

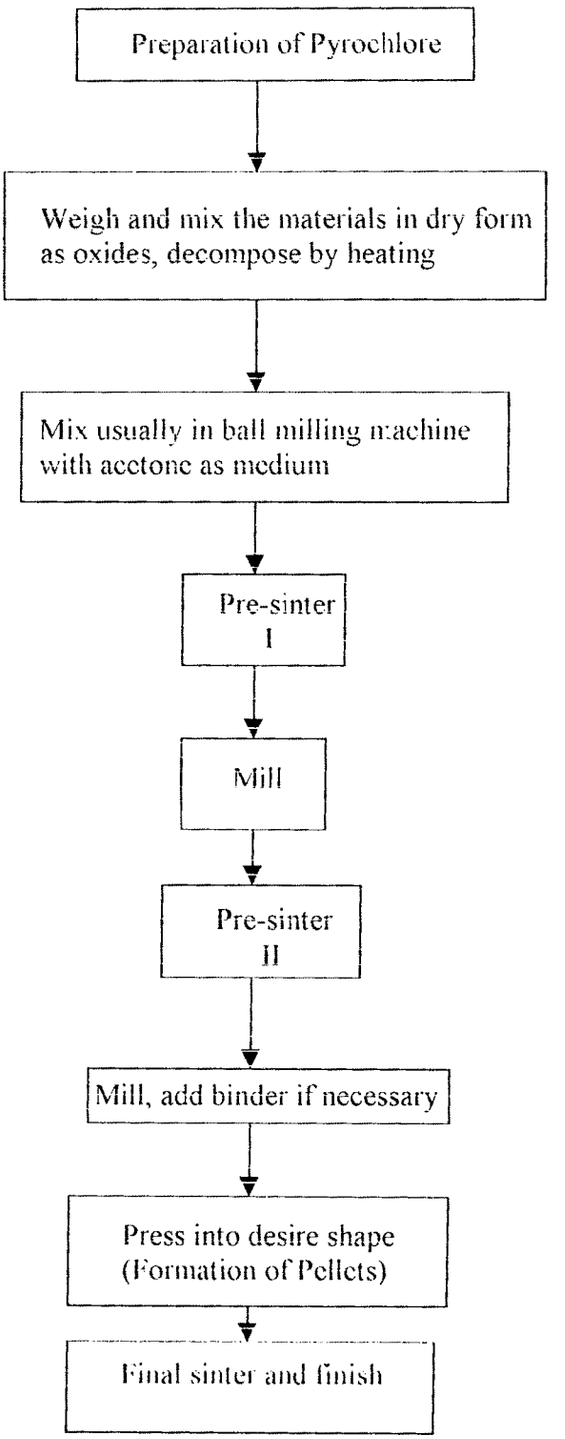


Fig.2.1:- Flow chart of Stages involved in preparation of pyrochlore by Ceramic dry method in Laboratory.

The powder mixture is presintered and then subjected milling. It is sintered again. Such powder undergoes the solid state chemical reaction easily at its reaction temperature.

**2.4 PRESINTERING: -**

The dry mixture is presintered at temperature of about 200°c -300°c below the final sintering temperature. According to Swallow et al (1),the purpose of the presintering or calcination is to

(a) decompose oxalates, carbonates and higher oxides, so that there is evolution of gas. This is essential because it is expected that there is no evolution of gases during the final sintering.

(b) assists homogenization of the material.

(c) reduce or control shrinkage during the final sintering.

(d) to reduce the effect of variations in compositions of raw materials.

Here the solid state chemical reaction is not the aim of the presintering. But it should be noted that the temperature at which presintering or calcination is carried out, the diffusivity of ions is sufficient to cause solid state chemical reaction to a small extent. The amount of reaction depends on the presintering temperature and the reactivity of the components.(2)

**2.5 MILLING AFTER PRESINTERING: -**

Milling of presintered powder involves reactivity as the small particle size is achieved. The milled powder is then used for preparing the final product of the required shapes.

**2.6 FINAL SINTERING: -**

Final sintering is the most common process of integrating and preparing solid state materials. To have best quality final product, the sintering must fulfil following requirements.

1) To bond particles together so as to import sufficient strength to the product.

2) To densify the grain compacts by eliminating (minimizing) the pores and

3) To homogenize the material by completing the solid state chemical reaction left unfinished in the presintering process.

As far as their mechanism is concerned the first two requirements are closely related.

The equation for the initial stage of the sintering process is given as -

$$\Delta L/L = [(AD\nu`V)\, t / (3\nu`_{av.}\, kT)]^{1/2} \qquad (2.1)$$

where, $\Delta L$ is the shrinkage of the compact.

V is the volume of single vacancy

D is coefficient of self-diffusion for the slowest moving species

$\nu`$ is surface energy

$\nu`_{av.}$ is the average radius of the particles

t is sintering time

K is Boltzman constant

T is absolute temperature at the time of sintering process.

A is the constant having approximate unity value

From equitation (2.1) it is clear that, the sintering fulfils first two requirements (requirement no a and b) more efficiently, when the compact features have high surface energy, high diffusivity and highly line particles.

We assume that the cations are present in current proportions, but the time and temperatures of sintering, the partial pressure of oxygen or any other sintering atmosphere and cooling rate affect them. During the sintering, densification and grain growth occur at the same time to lead variety of microstructures.

Volume diffusion is the main mechanism in ionic solids such as spinel. Nabarrow (3), Herring (4) theory for diffusion of micro creep is considered to be main mechanism for densification. The surface of pores acts as source of vacancies. Migration of vacancies occurs as a result of concentration gradient between curved surfaces of the pores and equilibrium vacancy concentration under the flat surface (Co). The vacancy concentration (Cr) under the surface of radius of curvature r is given by Kelvin equation.

$$Cr = Co \exp [\, 2r_s a^3 / r\, kT \,] \qquad (2.2)$$

where, $r_s$ is surface tension and $a^3$ is the vacancy volume.

As the concentration of grain boundary is equal to (Co), vacancy migrates at a temperature, where the mobility is sufficiently high from the pore surfaces to the grain boundaries. In grain growth, the grain boundary energy is decreased. When boundaries move to their center of curvature, the rate of grain growth (5) is given by.

$$D - Do = K\, t^n \qquad (2.3)$$

$$D = D + K\, t^n$$

where, Do is the particle size, K is temperature dependent factor and t is the time

The expected grain growth rate is proportional to $t^{1/2}$. However in practice it is proportion to $t^{1/2}$ due to the presence of impurities and inclusions in the grain boundaries, Zener (6) has given a purely empirical relationship for discontinuous grain growth.

$$D\,Cr = di/fi \qquad (2.4)$$

where di is diameter of inclusion and fi is the fraction volume.

The continuous grain growth may lead to a defect structure of giant grains in a matrix of small grains. This appears to be quite common in technical ceramics leading to a characteristically porous structure. It is because the rapid growth entraps pores in the grains, which is scarcely possible to eliminate due to their great distance from the grain boundaries. In order to maintain exact proportions of metal ions in the final product, careful control of sintering atmosphere is very important. Appropriate slow cooling is necessary so that material takes up the correct molecular structure as well as microcrystalline structure.

**2.7 GRAIN GROWTH: -**

The source of driving the grain growth is the grain boundary. As the grain size increases the energy of boundary decreases and the boundaries move towards the center of curvature. The presence of impurities in the grain boundaries hinders the grain growth. The grain growth occurs until the ratio of diameters of inclusion to the volume fraction is equal to the critical diameter of

grains when pores or inclusions disappears during heating the large grains are formed. The exaggerated grain growth occurs when average grain size reaches the critical size.

**2.8 DENSIFICATION AND POROSITY: -**

Porosity is a phase, which is always present in ceramic method of powder compact. To obtain low porosity (or high densification), it is useful to promote the sintering rate by using powder with large surface area. Larger pores will grow at the expense of small pores in its direct vicinity by volume or grain boundary diffusion of vacancies. However small pores moves along with moving grain boundary due to vacancy gradient over the two- pore surface. It has been found that at low rate of sintering, the pore growth becomes predominant and if it is discontinuous, grain growth is observed.

The microstructure with large pores ( related to compounds having low sintering rate) is achieved when the condition, $D_c C_c = D_o C_o$

is satisfied

where, $D_c$ is the diffusion constant of cation vacancies.

$D_o$ is the diffusion constant of oxygen vacancies.

$C_c$ is the bulk concentration of cation vacancies.

$C_o$ is the bulk concentration of oxygen vacancies.

**2.9 ACTUAL PREPARATION OF $Ce_{2-x}Nd_xTi_2O_7$ PYROCHLORE SAMPLES:-**

In present study, the samples were prepared by standard ceramic method using AR grade oxides. The starting materials used were, 1) $Ce_2O_3$ 2) $Nd_2O_3$ and 3) $TiO_2$.

The oxides of rare earth were weighed according to required mole proportions on semi-micro balance having least count of 0.001 gm. The Titanium oxide was weighed in same way, so as to mix with the rare earth.

$$Ce_2O_3 + 2\ Ti\ O_2 \rightarrow Ce_2Ti_2O_7$$

OR

The general balancing equation of chemical reaction.

$$A_2^{3+}O_3 + 2\ B^{4+}O_2 \rightarrow A_2^{3+}B_2^{4+}O_7$$

The gram molecular weights of these oxides are –

1) Gram molecular weight of $Ce_2O_3$ = 328.2287 gm. mole

2) Gram molecular weight of $Nd_2O_3$ = 336.4782 gm. mole

3) Gram molecular weight of $TiO_2$ = 79.8688 gm. mole

The oxides of Titanium and rare earth were mixed thoroughly in an agate mortar for 3-4 hours. The mechanical mixing was carried out carefully without any loss of powder and mixture was dried in an oven at a temperature of about $100^0$c. The dry mixture was then transferred into alumina crucibles and was presintered at 800 $^0$c, for 12 hrs, in air by using globar furnace. A chromel-alumel thermocouple was used for the measurement of temperature of the furnace. The samples were allowed to cool to room temperature slowly at the rate of 80 $^0$c per hour. The presintered powder was then taken in agate mortar and mechanical mixing is carried out once again for two hours and finally powder was collected in a clean tube.

About 1-2 gm. of presintered dry powder was taken in agate mortar and milled to have fine particles. This dry powder was then transferred into a die having 1.5cm diameter and pressed in a hydraulic press with the pressure of the

Table 2.1 Actual weights of different ingredients taken during the preparation (While taking weights, 4% of the molecular weight of each sample is taken)

| Sample no | X | Molecular weight | Weight of $Ce_2O_3$ | Weight of $2TiO_2$ | Weight of $Nd_2O_3$ |
|---|---|---|---|---|---|
| 1 | 0.0 | 487.9658 | 13.129 | 6.3895 | 0 |
| 2 | 0.2 | 488.791 | 11.816 | 6.3895 | 1.346 |
| 3 | 0.4 | 489.617 | 10.503 | 6.3895 | 2.692 |
| 4 | 0.6 | 490.441 | 9.19 | 6.3895 | 4.038 |
| 5 | 0.8 | 491.266 | 7.878 | 6.3895 | 5.384 |
| 6 | 1 | 492.091 | 6.565 | 6.3895 | 6.796 |

order of 8-10 tones per square inch about 5-10 minutes. After removing the load pellet was taken out from the die. Several pellets of different composition were prepared using the same technique.

The pellets thus prepared were placed on platinum foil in a glaobar furnace and final sintering was carried out at a temperature of 1100 $^0$c, about 24 hrs, in an air medium for the completion of solid state reaction. Then furnace was cooled at the rate of 80 $^0$c/hour. The pellets were polished and silver paste was pasted on both sides of the pellets for good ohmic contact. Some of pellets (in fact one pellet of each composition) were crushed separately in agate mortar. The powder of each composition is preserved and used to study x-ray diffraction pattern of product. Actual weights of different ingredients taken during preparation are reported in table 2.1

**2.10 X-RAY DIFFRACTION METHOD: -**

Atom of the solid substance acts as scattering centers for x-rays. The coherent scattering of x-ray is due to extranuclear electrons of the atoms and therefore intensity of scattered x-rays represents the number of electrons of the particular atom, which is responsible for scattering. Again in case of crystalline solids, the constituent atoms of the molecules are arranged with periodicity in space lattice. Periodicity in space along the chosen particular crystallographic co-ordinate axis is a constant called lattice parameter.

Diffraction maxima are found to occur only when the waves coming from two scattering centers are in phase and this condition is fulfilled provided that the Bragg's law is obeyed. In x-ray analysis a monochromatic x-radiation is allowed to fall on a certain crystal planes on which some atoms situated. If $\theta$ is

glancing angle and d is interplaner distance, then according to Bragg's law the diffraction maximum is obtained if

$$2d \sin\theta = n\lambda \qquad (2.6)$$

where, n is order of diffraction and $\lambda$ is wavelength of monochromic radiation

For cubic system, the distance between the two consecutive diffraction planes is given by

$$d = n\ [\ a^2 / h^2 + k^2 + l^2\ ]^{1/2} \qquad (2.7)$$

where a is lattice parameter, h, k, l are Miller indices and n is order of plane(7).

From equations (2.6) and (2.7) eliminating d we get

$$\lambda\ /2 \sin\theta = [a^2 / h^2 + k^2 + l^2\ ]^{1/2}$$

$$\lambda^2\ /4 \sin^2\theta = [a^2 / h^2 + k^2 + l^2\ ]$$

$$a^2 = (\lambda^2\ /4 \sin^2\theta\ )[\ h^2 + k^2 + l^2\ ] \qquad (2.8)$$

From equation (2.8), lattice parameter a can be calculated for cubic system. For this purpose, the Miller indices h, k, l of a particular plane responsible to produce diffraction maximum for the x-radiation of known wavelength are judicially decided. This process is called indexing of diffraction pattern.

The diffracting angle can be measured by rotating crystal method. In this method the crystal under investigation is introduced in the path of strictly monochromatic x-beam which gets reflected from the crystal planes. If the crystal is rotated very slowly through an angle $\theta$, then reflected beam under goes

the rotation twice that of θ. i. e. 2θ The reflected radiation is received in the ionization chamber and ionization current is detected and measured electronically in computerized x-ray diffractometer. If the angle of rotating crystal satisfies the Bragg's law, the diffraction maximum is obtained giving rise to sudden peak intensity in the direct current. The plot of angle of diffraction 2θ and the reflected intensity consists of several diffraction maximum satisfying the Bragg's law and such a record is called as diffractogram. The schematic diagram of x-ray diffractometer is shown in fig 2.2.

P. Debye and P. Scherrer (8) and A. W. Hull (9) replaced the rotating crystal method by the powder method in which finely divided powder of crystalline specimen is introduced in the path of monochromatic x-beam. Many microcrystollines are naturally and randomly oriented with all the angular distributions provided all over rotation in all angles. Maximum are produced at angles 2θ satisfying Bragg's condition which are detected by ionization chamber or a suitable counter mounted on a rotating goniometer in order to measure 2θ very accurately.

**2.11 EXPRIMENTAL: -**

For the present studies, the powder samples were scanned for x-ray diffraction on Phillips make computerized x-ray diffractometer PW-1710 using $Cuk_{\alpha}$ radiation, available in CFC of Shivaji University, Kolhapur. The diffraction angles varied between $10^0$ to $90^0$.

By considering predominant peaks on the pattern, the lattice parameters were determined for different samples. The planes (h k l) and correlated 'a'

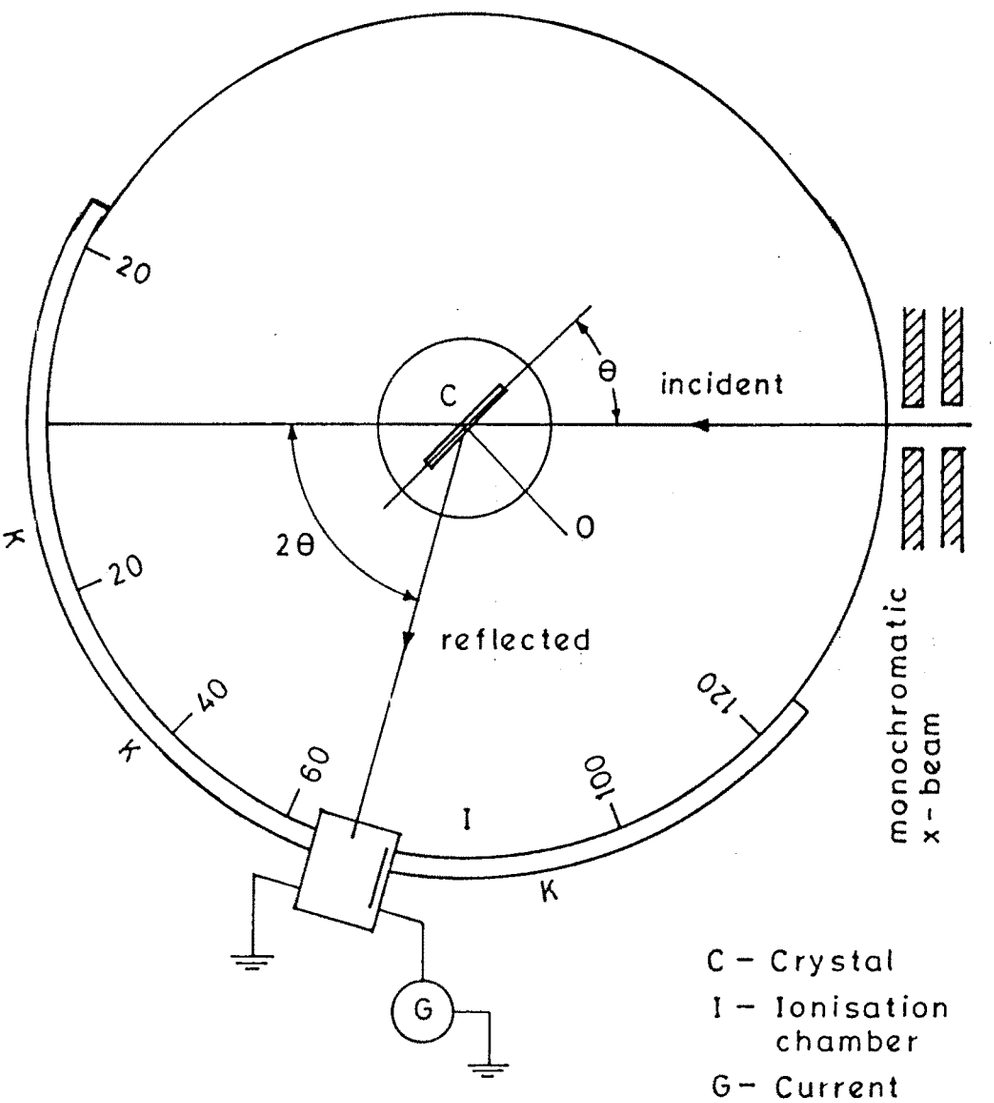


FIG. 2.2 SCHEMATIC, X-RAY DIFFRACTOMETER.

value thus obtained were used to calculate 'd' values which were then compared with 'd' values given directly by Bragg's law. The experimental interplaner spacing can be indexed as face centered cubic cell. Peak intensities and the systematic absences were typical of the pyrochlore structure.

**2.12 RESULTS AND DISCUSSION: -**

The x-ray analysis involves characterization and structure determination. In case of standard pyrochlore structure, having Fd3m ($O^h_7$) space group gives intense diffraction peaks for certain indices. Hence we may confirm the formation of pyrochlore if it exhibits the occurrence of their intense peaks for standard indices. In our present series, typical peaks (intensity maximum) pertaining to cubic pyrochlore structure do appear and this confirms pyrochlore compound. The standard FCC lattice of pyrochlores possesses the lattice parameter 'a' range from 10.38 to 10.80 $A^c$. The given planes for FCC system are (311), (222), (400), (331), (333), (440), (620), (622), (444), (642), (800), (662), (840) and (844).

X-ray diffraction pattern of all the pyrochlore samples namely x = 0.0, 0.2, 0.4, 0.6, 0.8 and 1 obtained by using monochromatic radiation at room temperature are shown in fig 2.3 to 2.8. The lattice parameter 'a' is calculated by using least square method. The calculated and observed d values along with the planes for all the samples are reported in tables 2.2 to 2.7. The observed and calculated lattice spacing (d values) are in good agreement for all the observed planes. The calculated lattice constants for all the samples are given in table 2.8. The lattice parameters lie in the range 10.7714 $A^0$ to 10.6768 $A^0$. It is observed

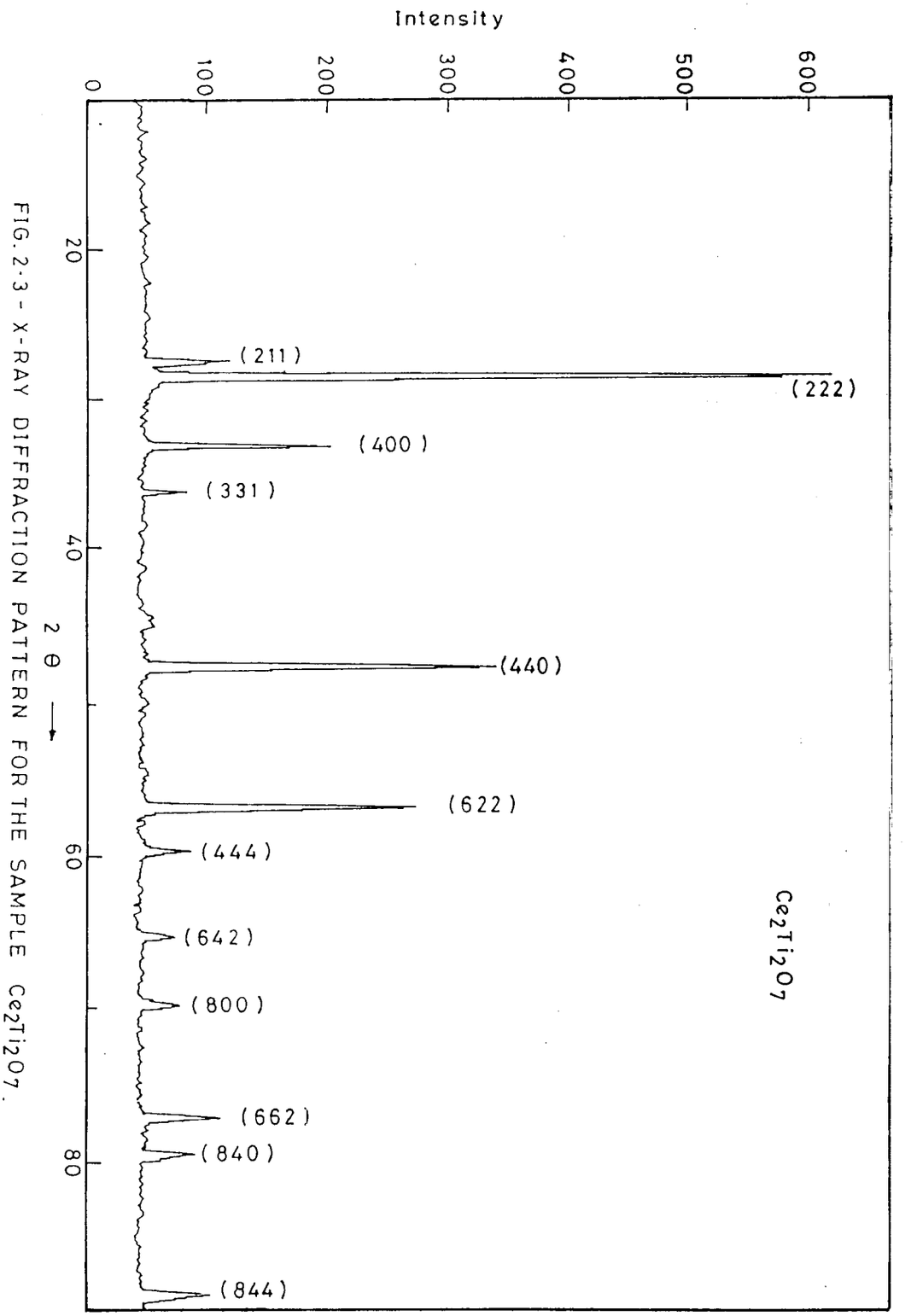


FIG. 2·3 - X-RAY DIFFRACTION PATTERN FOR THE SAMPLE $Ce_2Ti_2O_7$.

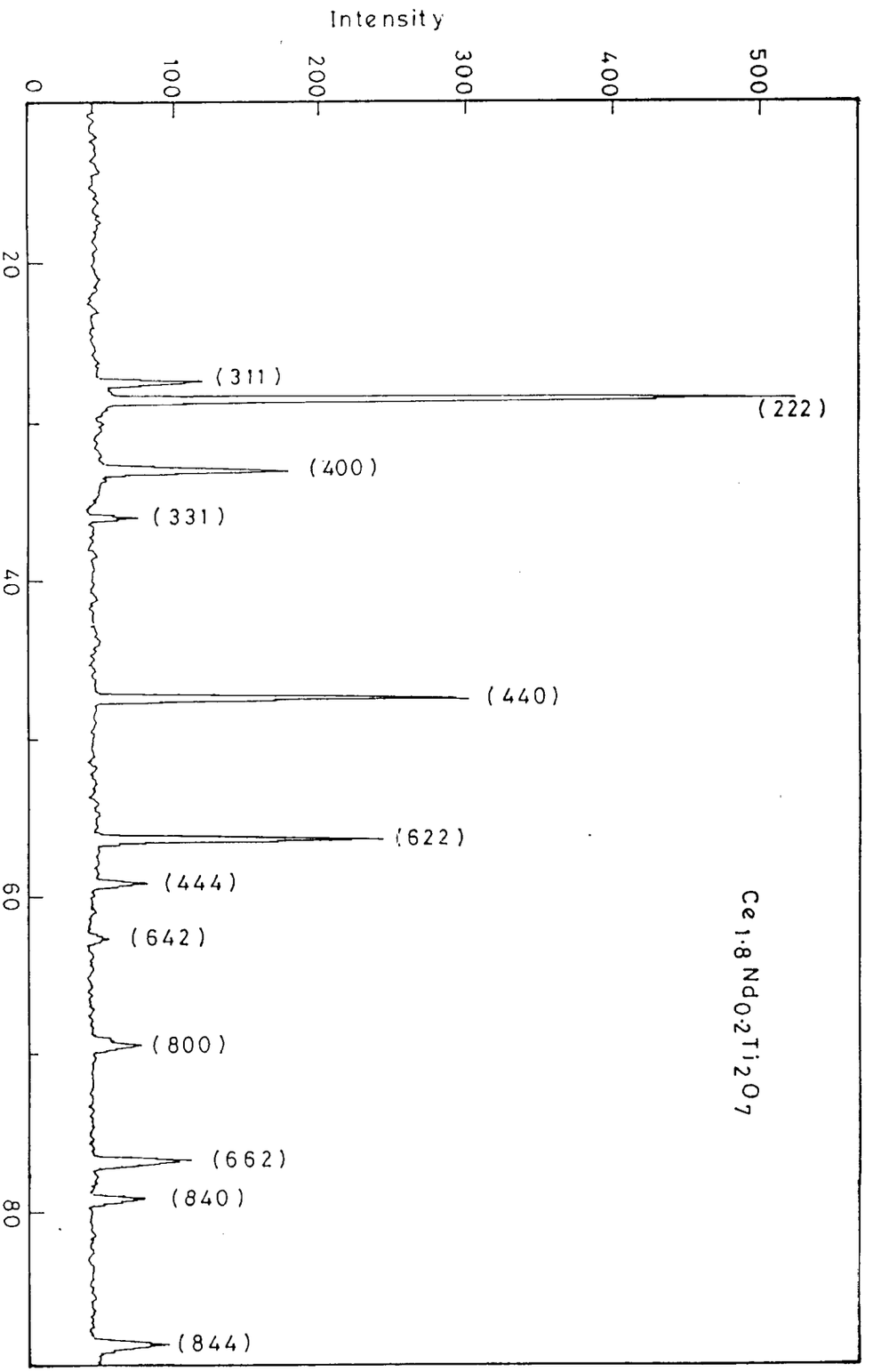


FIG. 2·4 – X-RAY DIFFRACTION PATTERN FOR THE SAMPLE $Ce_{1.8}Nd_{0.2}Ti_2O_7$.

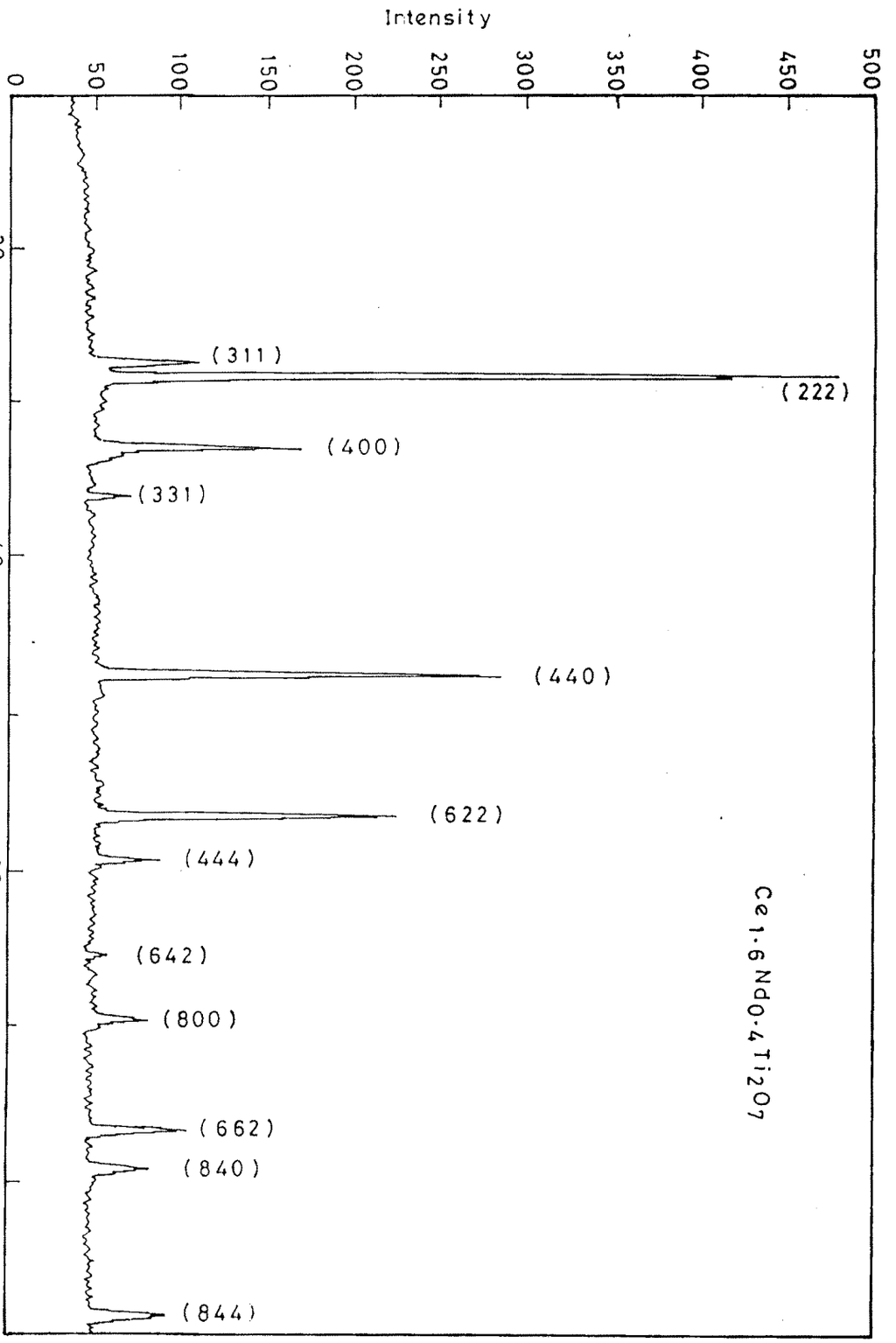


FIG. 2·5 – X-RAY DIFFRACTION PATTERN FOR THE SAMPLE $Ce_{1.6}Nd_{0.4}Ti_2O_7$.

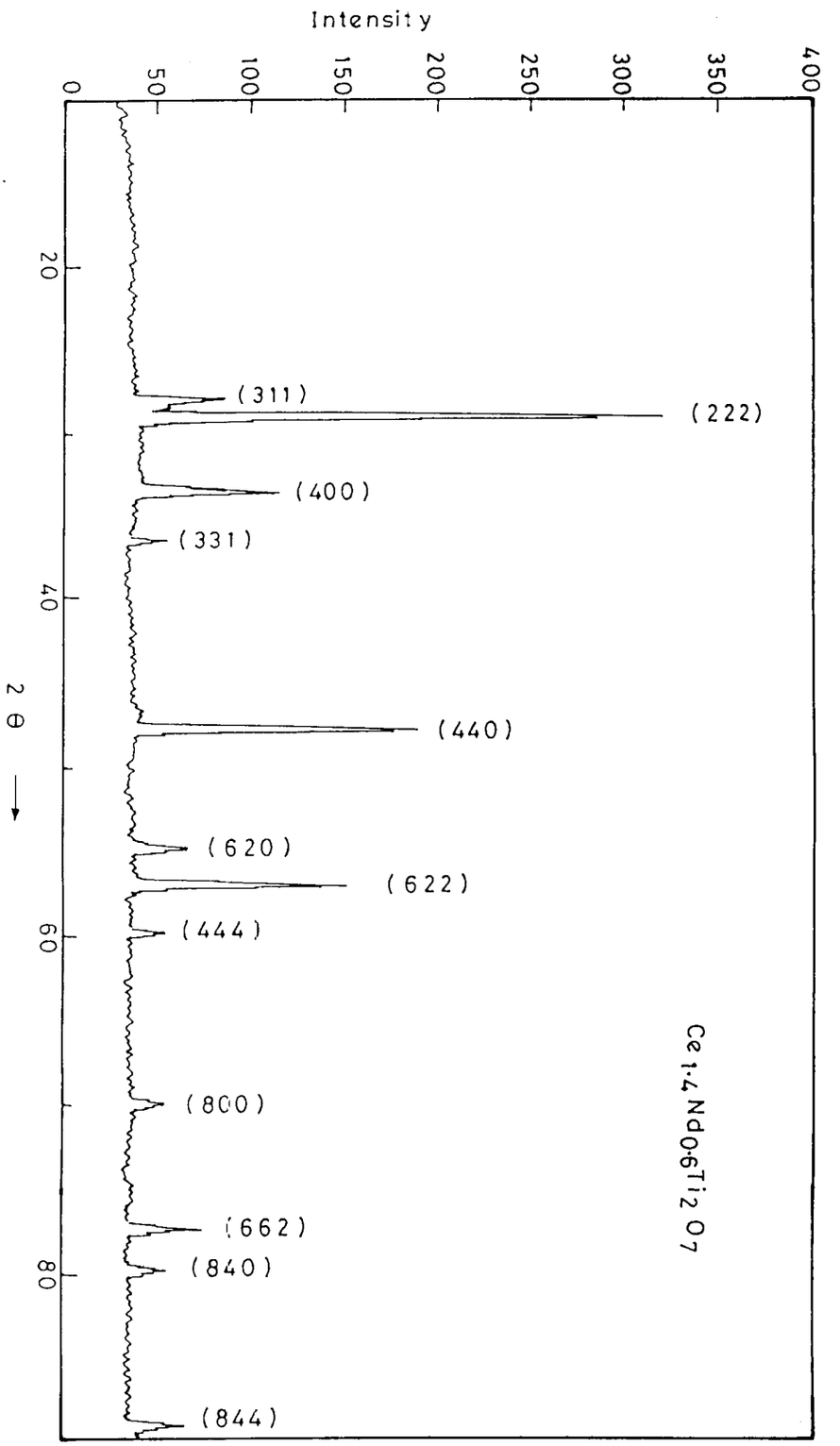


FIG. 2·6 – X-RAY DIFFRACTION PATTERN FOR THE SAMPLE $Ce_{1\cdot4}Nd_{0\cdot6}Ti_2O_7$.

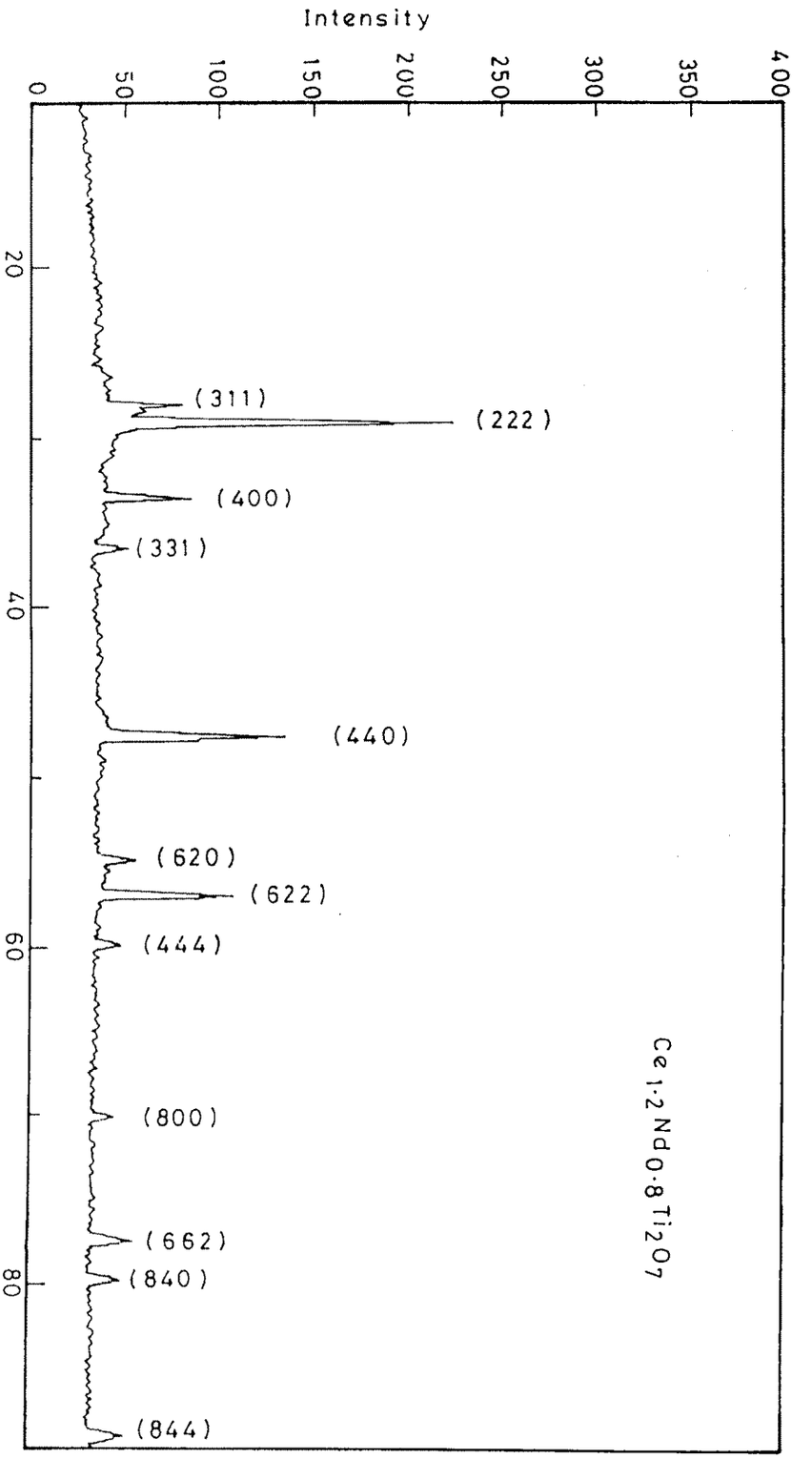


FIG. 2·7 – X-RAY DIFFRACTION PATTERN FOR THE SAMPLE $Ce_{1\cdot2}Nd_{0\cdot8}Ti_2O_7$.

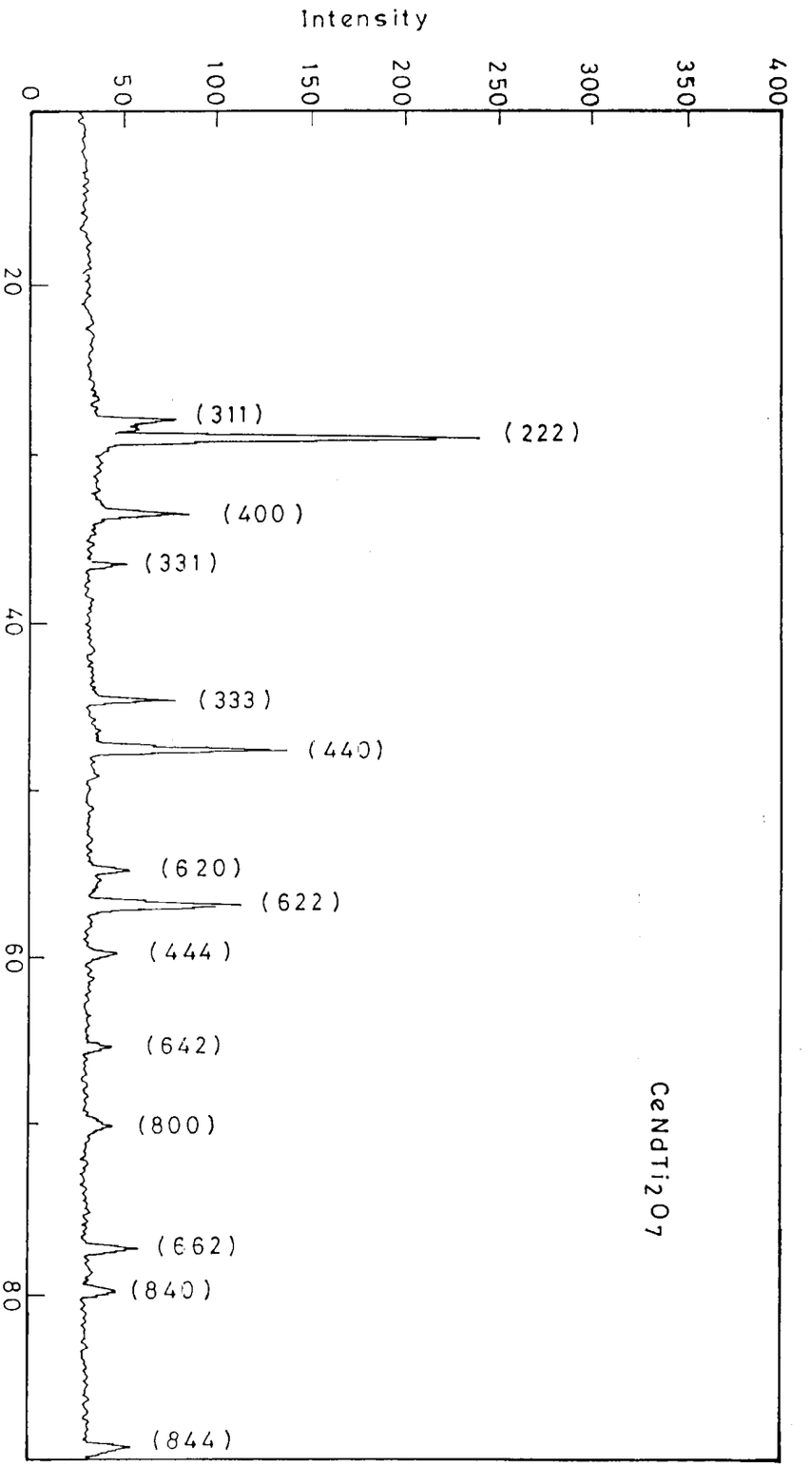


FIG. 2·8 - X-RAY DIFFRACTION PATTERN FOR THE SAMPLE $CeNdTi_2O_7$.

Table 2.2 MILLER INDICES AND hkl PLANES FOR

$Ce_2Ti_2O_7$

| h k l planes | d obs A° | d cal A° |
|---|---|---|
| 311 | 3.2368 | 3.2361 |
| 222 | 3.1085 | 3.1079 |
| 400 | 2.6951 | 2.6945 |
| 331 | 2.4788 | 2.4782 |
| 440 | 1.9083 | 1.9078 |
| 622 | 1.624 | 1.6237 |
| 444 | 1.5514 | 1.5511 |
| 642 | 1.4293 | 1.429 |
| 800 | 1.3479 | 1.3476 |
| 662 | 1.2352 | 1.235 |
| 840 | 1.2045 | 1.2043 |
| 844 | 1.1005 | 1.1003 |

Table 2.3 MILLER INDICES AND hkl PLANES FOR

$Ce_{1.8}Nd_{0.2}Ti_2O_7$

| h k l planes | d obs A° | d cal A° |
|---|---|---|
| 311 | 3.2305 | 3.2298 |
| 222 | 3.1064 | 3.1057 |
| 400 | 2.6927 | 2.6922 |
| 331 | 2.4761 | 2.4756 |
| 440 | 1.9071 | 1.9067 |
| 622 | 1.6266 | 1.6263 |
| 444 | 1.556 | 1.5557 |
| 642 | 1.4469 | 1.4466 |
| 800 | 1.3497 | 1.3494 |
| 662 | 1.2383 | 1.238 |
| 840 | 1.2074 | 1.2071 |
| 844 | 1.1026 | 1.1023 |

Table 2.4 MILLER INDICES AND hkl PLANES FOR

$Ce_{1.6}Nd_{0.4}Ti_2O_7$

| h k l planes | d obs $A^o$ | d cal $A^o$ |
|---|---|---|
| 311 | 3.227 | 3.2263 |
| 222 | 3.1032 | 3.1026 |
| 400 | 2.6904 | 2.6898 |
| 331 | 2.4755 | 2.475 |
| 440 | 1.9069 | 1.9065 |
| 622 | 1.622 | 1.6217 |
| 444 | 1.545 | 1.5541 |
| 642 | 1.4135 | 1.4132 |
| 800 | 1.3492 | 1.3489 |
| 662 | 1.2354 | 1.2352 |
| 840 | 1.2073 | 1.207 |
| 844 | 1.1026 | 1.1023 |

Table 2.5 MILLER INDICES AND hkl PLANES FOR

$Ce_{1.4}Nd_{0.6}Ti_2O_7$

| h k l planes | d obs $A^o$ | d cal $A^o$ |
|---|---|---|
| 311 | 3.1813 | 3.1806 |
| 222 | 3.0626 | 3.0619 |
| 400 | 2.6678 | 2.6672 |
| 331 | 2.4558 | 2.4554 |
| 440 | 1.9002 | 1.8998 |
| 620 | 1.6702 | 1.6698 |
| 622 | 1.6146 | 1.6143 |
| 444 | 1.545 | 1.5447 |
| 800 | 1.3414 | 1.327 |
| 662 | 1.2325 | 1.2323 |
| 840 | 1.2017 | 1.2014 |
| 844 | 1.0987 | 1.0984 |

Table 2.6 MILLER INDICES AND hkl PLANES FOR

$Ce_{1.2}Nd_{0.8}Ti_2O_7$

| h k l planes | d obs $A^o$ | d cal $A^o$ |
|---|---|---|
| 311 | 3.1796 | 3.179 |
| 222 | 3.0636 | 3.0629 |
| 400 | 2.6647 | 2.6641 |
| 331 | 2.4555 | 2.455 |
| 440 | 1.9034 | 1.903 |
| 620 | 1.6709 | 1.6705 |
| 622 | 1.6149 | 1.6145 |
| 444 | 1.5446 | 1.5513 |
| 800 | 1.3422 | 1.3304 |
| 662 | 1.2326 | 1.2323 |
| 840 | 1.2022 | 1.2019 |
| 844 | 1.0989 | 1.0986 |

Table 2.7 MILLER INDICES AND hkl PLANES FOR

$Ce_1Nd_1Ti_2O_7$

| h k l planes | d obs $A^o$ | d cal $A^o$ |
|---|---|---|
| 311 | 3.1807 | 3.1801 |
| 222 | 3.0564 | 3.0558 |
| 400 | 2.6628 | 2.6628 |
| 331 | 2.4552 | 2.4547 |
| 333 | 2.0251 | 2.0246 |
| 440 | 1.9053 | 1.9048 |
| 620 | 1.6696 | 1.6693 |
| 622 | 1.6136 | 1.6132 |
| 444 | 1.5426 | 1.5422 |
| 642 | 1.4247 | 1.4244 |
| 800 | 1.346 | 1.3403 |
| 662 | 1.2329 | 1.2327 |
| 840 | 1.1999 | 1.1997 |
| 844 | 1.0982 | 1.098 |

that lattice constant decreases with increase in Nd value. This is due to fact that with decreasing in ionic radius of content lattice parameter decreases.

All the atoms in the pyrochlore unit cell occupy special positions with space group Fd3m. For $A_2B_2O_7$ these positions are given in table 2.10.

The displacement of oxygens and the bond lengths can be calculated by x-ray analysis. The bond lengths are calculated by taking ideal values of x = 0.3125 or 5/16 for regular octahedra and u = 0.375 or 5/8 for regular cube. Generally oxygen 'x' parameter is found to range from 0.39 to 0.355 (with B-O ion chosen as origin).

By using relation

$$B\text{-}O = a\,(u^2 - u + 9/32)^{1/2} \qquad (2.9)$$

$$A\text{-}O = a\,[(u + x + 1/2)^2 + 2\,(1/8 - x)]^{1/2} \qquad (2.10)$$

The bond lengths are calculated. The calculated bond lengths(A-O and B-O bond lengths) are shown in Table 2.8. The A-O bond lengths lie in the range from 3.4986 A° to 3.4678A°. Similarly the B-O bond lengths lie in the range from 2.332 A° to 2.3115 A°.

The density of samples can be determined by measuring both weight and volume of the samples, but it gives some error, so liquid immersion method have also been used to calculate the correct density of the sample. Handrick and Jefferson (10) have developed a method to measure the density accurately. This method depends on immersing the solid in some liquid of known density in which the solid is completely insoluble. For this measurements liquid piknometer was used. It was designed by Johnson and Adams (11). In the

Table2.8:- Lattice constants and bond lengths for all samples $Ce_{2-x}Nd_xTi_2O_7$

| Composition | a A° | B-O A° | A-O A° |
|---|---|---|---|
| x = 0.0 | 10.7714 | 2.332 | 3.4986 |
| x = 0.2 | 10.7652 | 2.3306 | 3.4965 |
| x = 0.4 | 10.7536 | 2.3281 | 3.4927 |
| x = 0.6 | 10.6848 | 2.3132 | 3.4704 |
| x = 0.8 | 10.6801 | 2.3122 | 3.4689 |
| x = 1.0 | 10.6768 | 2.3115 | 3.4678 |

Table 2.9:-Physical Constants of $Ce_{2-x}Nd_xTi_2O_7$

| Composition | Mol.weight gm-mol. | X-ray density dx gm/cc | Sample density ds gm/cc | Porosity p % | Particle size t µm |
|---|---|---|---|---|---|
| x = 0.0 | 487.993 | 6.1511 | 5.7993 | 6 | 0.136 |
| x = 0.2 | 488.817 | 6.1768 | 5.8504 | 5 | 0.091 |
| x = 0.4 | 489.641 | 6.2156 | 5.8137 | 6 | 0.117 |
| x = 0.6 | 490.465 | 6.2665 | 5.2696 | 16 | 0.102 |
| x = 0.8 | 491.289 | 6.2487 | 5.6027 | 10 | 0.102 |
| x = 1.0 | 492.113 | 6.2783 | 5.2313 | 17 | 0.104 |

Table 2.10:- Special position with space group Fd3m of the $A_2B_2O_7$ Pyrochlores

| Ion | Location | Site symmetry |
|---|---|---|
| 16 A | 16d | 3 m ( D3d) |
| 16B | 16c | 3 m (D3d) |
| 48O | 48f | mm ( C2v) |
| 8O` | 8b | 4 3m (Td) |

pyknometric method, the volume of the solid was more accurately found by determining the changes in weight.

The fundamental equation for the calculation of sample density ds of solid is

$$ds = Ws / VdL \qquad (2.11)$$

where Ws is weight of solid of volume VdL. VdL can be regarded as the amount of liquid (VdL in gm of density dL) which would be displaced in gm of solid were put in to a complete liquid filled vessel.

The densities of all the samples were measured by liquid immersion method described above. For this measurement, water is used as a liquid (The present samples are insoluble in water). The measured densities are given in Table 2.9.

The porosity P of each sample was obtained by using equation.

$$P = [(dx - ds)/dx]\ 100 \qquad (2.12)$$

And

$$dx = 8\ M / N\ a^3 \qquad (2.13)$$

where, ds is the actual density calculated by liquid immersion method, M is molecular weight, a is the lattice parameter and N is Avagardro's number. The values of porosity are listed in Table 2.9. It is observed that these samples are of almost same porosity and it is less than 15 %.

The average particle size for the samples is also listed in Table 2.9, which is obtained by using equation

$$t = 0.9\ \lambda / B \cos\theta \qquad (2.14).$$

Where $\lambda$ is wavelength of monochromatic x-beam, B is half width maximum. It is observed that these samples are of nearly same size of 0.1 $\mu$m.

## REFERENCES


(1) Swallow D. and Jordon A.K., Proc. British Ceram. Soc. 2, **1** (1964)

(2) Sato T: ITEE Trans. Mag. Mater 6, **795** (1970)

(3) Nabarrow F.R.N. Rept. Conf. Strength of Solids,
Phys Soc. London **75** (1948)

(4) Herring C; J. Appl. Phys. 21, **437** (1950)

(5) Burke J.E. "Kinetics of High temperature Processes",
Edi W.D.Kingery N.Y. **109** (1959)

(6) Zener C. Smith C.S. Trans AIME 175, **15** (1948)

(7) Cullity B.D. "Element of X-ray Diffraction"
Addison Wesley Publishing Co. INC England (1959).

(8) Debye P. Sc. Scherrer P, Physik 2, 17, **277** (1916).

(9) Hull A.W. Phys. Rev. 9, 84, **564** (1916)
and Phys Rev. 10, **661** (1917).

(10) M.A.Subramanian, G.Aravamudan and G.V.Subba Rao. Prog. Solid St. Chem. 15, **58** (1983).

(11) Hendricks S.B. and Jefferson M.E.; J. Opti. Soc. 23, **299** (1933)

(12) Johnson and Adams L.H, J Am. Ceram. Soc. 34, **563** (1912).